17th IMEKO TC 10 and EUROLAB Virtual Conference
"Global Trends in Testing, Diagnostics & Inspection for 2030"
October 20-22, 2020.

Diagnostics of the RIAA Equalizer in a Turntable Using Artificial Neural Network

Grzegorz Makarewicz[1], Piotr Bilski[2]

[1]*Institute of Radioelectronics and Multimedia Technology, Warsaw University of Technology, Warsaw, Poland, G.Makarewicz@ire.pw.edu.pl, +48 222347748, pbilski@ire.pw.edu.pl, +48 222347644*

***Abstract* – The following paper presents the methodology of RIAA equalizer condition analysis based on measurements of its amplitude and phase characteristics. The RIAA equalizer is used during the signal recording and is an integral part of modern turntables. It's parameters determine the quality of the music being played. The task is to determine the critical values of electronic components (capacitors) based on the characteristics of signals observed at the circuit's output. It is considered difficult due to the presence of noise, elements' tolerances, and simultaneous drift of several system's parameters. The presented methodology uses the Artificial Intelligence (AI) module that implements the task of parameter identification. The knowledge exploited by the AI-based module is extracted during machine learning, based on the dataset obtained during the simulations of the equalizer's computer model. For the decision-making module, the standard tool for the regression tasks, i.e. RBF-type Artificial Neural Network (ANN) was used. The obtained results allow for considering the potentially high usefulness of the presented approach for the parameters identification in electronic circuits used in audio technology.**

Keywords – RIAA correction, turntable, neural network, artificial intelligence, machine learning.

I. INTRODUCTION

Despite the quickly advancing technological progress and hardware-based digital signal processing methods, analog circuits are still used in specific audio equipment. The recent return of the analog music (in the form of the vinyl disc) is both surprising and posing a recurring challenge for the diagnostic domain. The quality of the sound reproduced with this type of equipment is, from the point of view of subjective feelings (depending on the type of music played), often perceived as much better than that obtained with digital devices. This advantage, especially appreciated in the audiophile community, is considered by manufacturers of audio devices using analog signal processing technology. It therefore requires extremely high-quality elements (capacitors, resistors, amplifiers) with low tolerances (even below 1%), which makes them expensive. In most cases, the analog audio systems (correctors, preamplifiers, amplifiers) are discrete, which in connection with their high costs makes them an important target not only for fault detection, but also identification and location of these failures.

One of the most important components in the analog electroacoustic track is the gramophone, equipped with the phono cartridge allowing for playing the music recorded on the vinyl plate. The method used to create a long-playing disc affects the frequency parameters of the recorded music material. They are represented by the RIAA correction curve. Established in 1954 by the Recording Industry Association of America, it is a standard valid to this day. Consequently, the way the sound is stored on the carrier requires applying the normalized frequency correction. The playback system must be then also equipped with the proper corrector [1]. When it is implemented as the electronic circuit using traditional analog elements for music processing, its parameters depend on their physical characteristics. Therefore, during the design of the correcting module, the effects of changing the circuit parameters due to the temperature changes or passage of time (for instance, by wearing them out), should be considered. The main tool for monitoring of such a system is the frequency characteristics analysis., which allows for evaluating particular spectral components on the output of the corrector, where the response to the excitation is measured [2].

To obtain the desired frequency characteristics for the corrector, the specific filter configuration must be prepared. For that purpose, internal electronic elements (resistances and capacitances) must be selected and their values determined. Depending on the used methodology, it is then possible to design the corrector circuit that is more or less resistant to unfavourable factors (like noise and interfering signals) affecting its operational parameters. It is also important to determine the actual state of the circuit, i.e. whether it still operates correctly, according to the design specifications, or is it already

faulty. As the most RIAA equalizers are still implemented as discrete analog circuits, in the latter case the source of the problem should be replaced with its new counterpart.

The Artificial Intelligence (AI) approaches can be used to design the diagnostic system, enabling the fault detection and classification based on the available data [3]. These are used to train the classification or regression machine. In most cases, the data sets contain measurements crucial for determining the source, intensity of the fault and (preferrably) the actual parameters' values. The data is in most cases obtained from circuit models simulated in the specialized software, as introducing faults into the actual audio system would be too costly.

The aim of the paper is to present the method for the on-line diagnostics of the analog audio RIAA correction filter. The Radial basis Function Artificial Neural Network (RBF ANN) was used to identify selected parameters (i.e. capacitances) of the designed circuit model. The implemented method was trained on the data sets extracted from the model simulations. The obtained results prove the Parameter Identification (PI) task can be implemented for such a circuit with acceptable accuracy.

The paper structure is as follows. In Section 2 the RIAA correctors are introduced. Section 3 presents the applied circuit PI method based on the RBF ANN. In Section 4 experimental results are shown where the dependency between the configuration of the ANN and the obtained accuracy is shown., Section 5 covers conclusions and future prospects.

II. RIAA CORRECTION CIRCUITS

Production process of the vinyl music disks imposes the usage of the correction circuits. The frequency correction is used during the sound processing, closely related to the recording technology. Its parameters are presented in the transmittance (1), where *F(s)* is the transfer function of the correction filter in the Laplacean domain of the complex variable *s*, T_1, T_2 and T_3 are normalized time constants, determining properties of the filter.

$$F(s) = \frac{(s \cdot T_1 + 1)(s \cdot T_3 + 1)}{(s \cdot T_2 + 1)} \qquad (1)$$

Characteristics of the filter used during the sound playback is the mirror reflection of the characteristics applied for sound recording [2]. Both patterns for the analog disks are presented in Fig. 1: the dotted line represents the recording, while the continuous one stands for the playback. Both lines intersect in the middle of the audio frequency range (i.e. 1kHz).

To correctly play the content of the disk, the electroacoustic track must have the adjusted corrector in the form of filter. Such filters, according to the RIAA standard, are either active or passive. The latter are made of only passive elements (resistors and capacitors). Active filters contain additional elements such as transistors or operational amplifiers. The advantage of passive filters, appreciated by audiophiles, is the lack of noise and distortions introduced by active elements. In the period of the greatest popularity of vinyl disks, the former were used. Their advantages, thanks to the negative feedback loop, included stability of the circuit parameters and low sensitivity for elements' changes. Currently in the analog electroacoustic circuits, the passive RIAA filters are used, inserted in the audio track. In this case the accurate selection of the elements is crucial, as any changes in their values significantly influence the played sound quality.

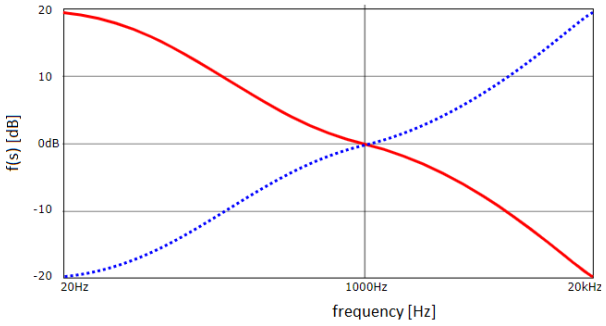

Fig. 1. Frequency characteristics of the recording (dotted curve) and playback (continuous curve) correction filters

Example of the modern passive filter, treated in the presented research as the System Under Test (SUT) is presented in Fig. 2. It contains six capacitors and resistors configured to provide the amplitude and phase characteristics ensuring the fulfilment of the requirements defined by the relation (1) and illustrated in Fig. 1.

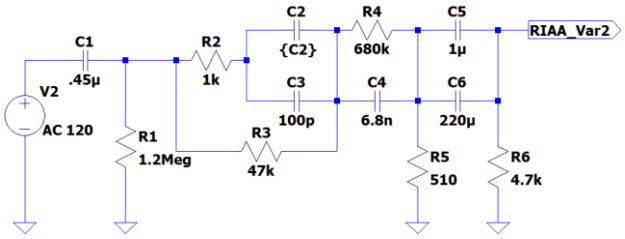

Fig. 2. Schematic diagram of the passive correction filter

The structure of the circuit reflects the actual construction requirements. For instance, as there is no single capacitor with capacity of 221µF, it is represented by two elements, C_5 and C_6 (of capacitances, respectively, *220µF* and *1µF*). Therefore, there is no point in diagnosing the latter, as even its significant deviations are too small to be noticed on the output. The same situation is with capacitors C_2 and C_3. Similarly, C_1 (with nominal capacity of *470nF*) is only used to cut off the DC component, so it also has been excluded from experiments. The remaining diagnosable elements have the following nominal values: C_2=*1.5nF*, C_3=*100pF*, C_4=*6.8nF*, R_1=*1MΩ*, R_2=*1kΩ*, R_3=*47kΩ*, R_4=*680kΩ*, R_5= *510Ω* and R_6=*4.7kΩ*.

Amplitude and phase characteristics are obtained after exciting the SUT with the sinusoidal pattern with the amplitude of 100mV and frequency ranging from 20Hz to 20kHz. The model of the circuit was created and tested in the LTSpice software [4].

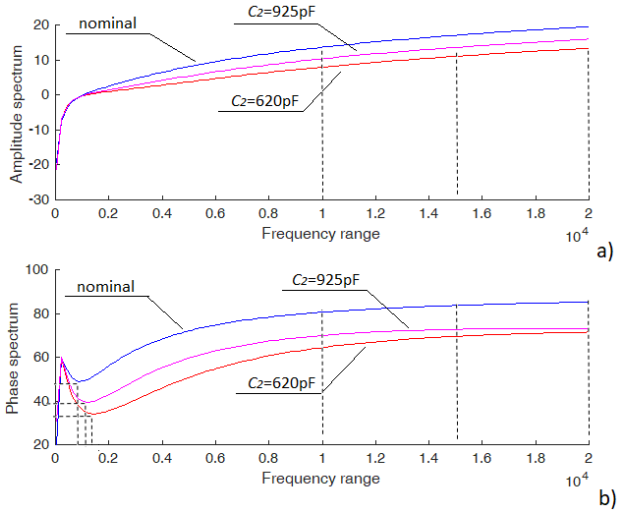

Fig. 3. Amplitude (a) and phase (b) characteristics of the correction filter for various values of the capacitor C_2 (other parameters nominal)

The experimented presented in the paper are aimed at determining deeper knowledge about the possibility of the presented SUT's PI based only on the frequency characteristics (fundamental tool for the acoustic circuits analysis) obtained at the output node (see Fig. 2). Although all elements are considered for identification, it is expected that only their subset will be diagnosable (already mentioned capacitors C_1, C_6, resistor R_1). Tolerances of nominal parameters are low, therefore, assuming their sensitivity is high enough (changes are visible on the output), any deviation should be detectable by the diagnostic system. Characteristics presented in Fig. 3 are the source of diagnostic features for the ANN-based system.

III. RBF ANN-BASED SUT PARAMETER IDENTIFICATION

In the modern diagnostics applications, AI-based methods are the standard solution [5]. The aim of such an approach is to determine the state of the SUT (either as the discrete categories in the case of fault detection or identification [6], or the real numbers, indicating the actual values of the diagnosed parameters [7]) based on the set of symptoms (or attributes), observed in the circuit's response. The aim of the presented research was to determine the actual values of the SUT parameters, which requires solving the regression task.

The architecture of the PI module is presented in Fig. 4. It consists of three subsequent steps: measurement data (frequency characteristics) collection, extraction of features from them and forming input vectors for the regression algorithm. The crucial step for the AI-based module is the preparation for training data, from which knowledge about the SUT's state can be inferred. Although the architecture itself is generic and could be employed to monitor other circuits, the key issue is the analysis of the SUT's structure to identify the most challenging faults and adjusting the regression machine characteristics. This is be done for each SUT individually.

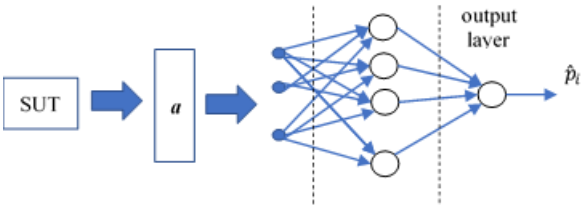

Fig. 4. The RBF ANN for approximation for all capacitors' values

The following features were selected (in Fig. 3 indicated by vertical dotted lines) from the amplitude and phase characteristics:

- amplitude values of the peaks at 10kHz, 15kHz and 20kHz,
- minimum phase value and its frequency,
- phase values at 10kHz, 15kHz and 20kHz.

These symptoms were identified as bearing enough information to make the regression of all diagnosable elements possible.

A. Data set characteristics

The AI-based approaches require data sets to extract knowledge and further use it to evaluate actual values of parameters. The set contains vectors of symptoms, extracted from the simulated SUT responses after setting the desired parameters' values. In this way it is possible to perform the supervised learning for the selected regression machine.

During simulations, tolerances of used elements were considered. Even in the nominal state, the SUT elements had values randomly disturbed with the uniform distribution. The tolerance margins were set to 5% (in both directions) of the values provided by the designer (which is the maximum reasonable value for the high-quality equipment). Generation of the data set consisted in repeated circuit simulations after introducing the single fault into the structure (including the nominal state). Each capacitor was represented by 11 simulations for its value deviating up to 90% from the nominal state (in both directions). The experiments were performed only for the single fault (i.e. with one selected parameter being the problem and all other within tolerance margins). This gives the data set D (2) with $n=132$ vectors containing $m+k=15$ values each (m=8 attributes a_i – and $k=12$ actual values of the diagnosed elements p_j).

$$D = \begin{bmatrix} a_{11} & \cdots & a_{1m} & p_{11} & \cdots & p_{1k} \\ \vdots & \ddots & & \vdots & \ddots & \vdots \\ a_{n1} & \cdots & a_{nm} & p_{n1} & \cdots & p_{nk} \end{bmatrix} \quad (2)$$

After creating the set D it had to be divided into two subsets: L for training the regression machine and T for testing it. During the cross-validation, the set D was repeatedly divided into two subsets in the relation 5:1, both representing the same amount of symptoms vector for each capacitor. This way each set L contained 108 examples, while the set T – 24 examples.

B. Regression algorithm

In the regression task the RBF ANN was used. It is the simple neural network aimed specifically at approximating real-valued functions. Its structure contains the single hidden layer with adjustable number of neurons. The network is the well-established tool in the diagnostics [8]. It was selected in the contrast to deep learning architectures, which have proven the most successful, but require large amounts of data [9]. The conducted experiments assumed the size of data sets is limited (as described in section III.A), so another outcome is knowledge about the capacity of the RBF-ANN trained on small data sets.

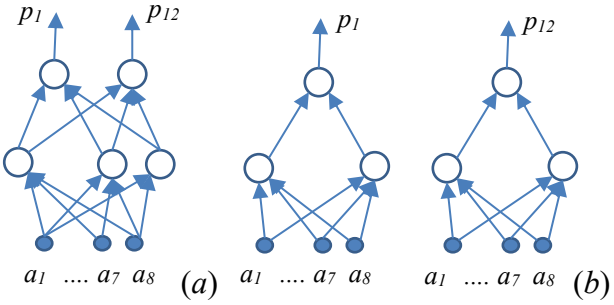

Fig. 5. Architectures of the RBF ANN for the parameter identification: single network (a), multiple networks (b)

In the presented research two variants of the diagnostic module were prepared. The first one is a single network approximating all parameters (further called Single Network Approximator - SNA). The second approach is the separate network for each parameter approximation (further referred to as Individual Network Approximator - INA). Structures of such networks, are presented in Figure 5, consists of two layers: hidden with the Gaussian (RBF) activation functions and the output one, with the linear activation function. The number of inputs depends on the number of symptoms in the vector ***a*** (here *9*). The number of neurons in the hidden layer is adjustable during the design and training of the network and was the optimized parameter during our research. The produced value of the *i*-th parameter's $\hat{p}_i$ estimation is confronted against its actual value p_i during the regressor training (to adjust the weights' values). The ANN architectures were implemented in the Matlab environment, using the Artificial Neural Networks toolbox.

The training efficiency is evaluated using the Mean Square Error (MSE), for the single evaluated parameter (p_i) measured as follows:

$$MSE(p_i) = \frac{1}{|L|} \cdot \sum_{j=1}^{|L|} \left(p_{ij} - \bar{p}_{ij}\right)^2 \quad (3)$$

where $\bar{p}_{ij}$ is the average value of the *i-th* parameter. The overall MSE (used during training the combined network from Fig. 5a) is the sum of particular errors for each output.

The regression quality during the testing is measured for each element separately, using the normalized score (4) [10]. Its usage is preferred when multiple various parameters are approximated, as efficiency of different regression modules can be compared. Here p_{ij} is the actual value of the *i-th* SUT parameter for the *j-th* symptoms vector from the set, $\hat{p}_{ij}$ is its estimated value and $\bar{p}_{ij}$ is the average of the actual values. The maximum value of the accuracy is *1*, therefore the approximation is practically usable if $acc(p_i)>0.5$. Negative values mean the approximation outcome is useless.

$$acc(p_i) = 1 - \frac{\sum_{j=1}^{n} \left(p_{ij} - \hat{p}_{ij}\right)^2}{\sum_{j=1}^{n} \left(p_{ij} - \bar{p}_{ij}\right)^2} \quad (4)$$

IV. EXPERIMENTAL RESULTS

The presented diagnostic system was trained and tested on data sets collected from the RIAA filter simulations. Experiments included verification of ANN hyperparameters, including the number of neurons in the hidden layer and the width of the Gaussian curve operating as the activation function. Both architectures from Fig. 5 were also compared

A. Parameter identification efficiency

The first experiment was aimed at determining if it is possible to train RBFANN for the accurate PI task in conditions described in Section II. Initially, the INA configuration was tested as considered the safer one (for each parameter the weights were adjusted separately). This requires creating 12 networks, training them on the set L and determining their generalization ability using the set T. During the training it was important to observe MSE, as if its value was high (i.e. not lower than *0.1*), the regression machine was probably unable to follow parameter changes. This could also be confirmed while observing the convergence of the training process. The best results obtained for capacitors and resistors are in Table 1 and 2, respectively, where MSE is the squared unit of the subsequent quantity (either resistance or capacitance).

Values in both tables are averages for 5 cross-validation trials. Networks for capacitors C_5 and C_6 and resistor R_1 were not trained correctly, which suggests their performance on the testing set may be low.

Table 1. Training results for capacitor-identification RBF-ANN.

Parameter	C_1	C_2	C_3
MSE	1.33e-3	7.12e-11	2.59e-10
Parameter	C_4	C_5	C_6
MSE	2.0e-17	7.8e+3	2.81e+2

Table 2. Training results for resistor-identification RBF-ANN.

Parameter	R_1	R_2	R_3
MSE	75.72	1.31e-14	2.76e-17
Parameter	R_4	R_5	R_6
MSE	4.34e-6	4.21e-10	1.71e-10

Tables 3 and 4 show approximation results for subsequent parameters. The worst results are for elements C_1, C_5, C_6, R_1 and R_4 , which confirms their poor training outcomes. It also indicates that MSE obtained during the training is a good prognostic for the generalization ability, The proposed method is useful to monitor multiple parameters (especially resistors), but to improve its accuracy, the amount of data must be increased. The second idea is to increase the amount of symptoms collected from new accessible nodes or by adding the analysis domain. Incorporation of the measurable nodes is easy in this case, as the circuit is discrete and all nodes are available for use.

Table 3. PI results for capacitor-identification RBF-ANN.

Parameter	C_1	C_2	C_3
acc	-1.89e-1	0.63	1.01e-2
Parameter	C_4	C_5	C_6
acc	-9.38e-1	-3.45	-3.44

Table 4. PI results for resistor-identification RBF-ANN.

Parameter	R_1	R_2	R_3
acc	-2.85e-1	0.54	0.98
Parameter	R_4	R_5	R_6
acc	-1.95e-1	0.58	-3.4e-2

B. Optimization of the RBF ANN-based regression

The most important parameter of the network is the number of neurons $|N|$ in the hidden layer, strongly depending on the size and complexity of available data. During the training, neurons are subsequently added to improve the MSE until their maximum number (equal to the number of examples in the set) is reached. Observation of this parameter allows for evaluating the training efficiency (especially regarding convergence of the process).

The design aims at determining the minimum number of neurons ensuring the acceptable accuracy. Example of the training process for the capacitor C_1 is presented in Fig. 6. The optimal number of units here is 90. Repeating experiments for all networks (aimed at approximating values of subsequent parameters) allowed for determining the optimal number of neurons, i.e. the minimal number ensuring the maximum possible accuracy. Results for capacitor-aimed ANNs are in Table 5, while their counterparts for resistors – in Table 6. In the case of C_5 and C_6 the convergence was very slow, stopping at 50 neurons. The same was for the resistor R_1. This is in line with low MSE values of these elements (see Table 1 and 2). Example of the training process for R_1 is in Fig. 7.

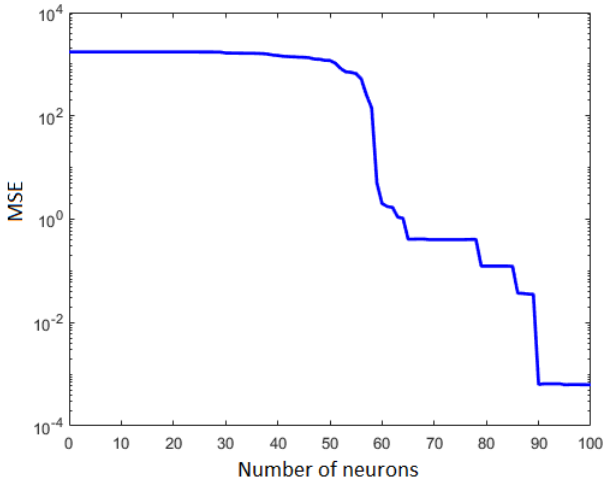

Fig. 6. Dependency between the number of neurons and MSE (capacitor C_1)

Table 5. Optimal number of neurons for capacitor-identification RBF-ANN.

Parameter	C_1	C_2	C_3	C_4	C_5	C_6
$\|N\|$	100	104	104	105	50	50

Table 6. Optimal number of neurons for resistor-identification RBF-ANN.

Parameter	R_1	R_2	R_3	R_4	R_5	R_6
$\|N\|$	105	90	100	98	96	88

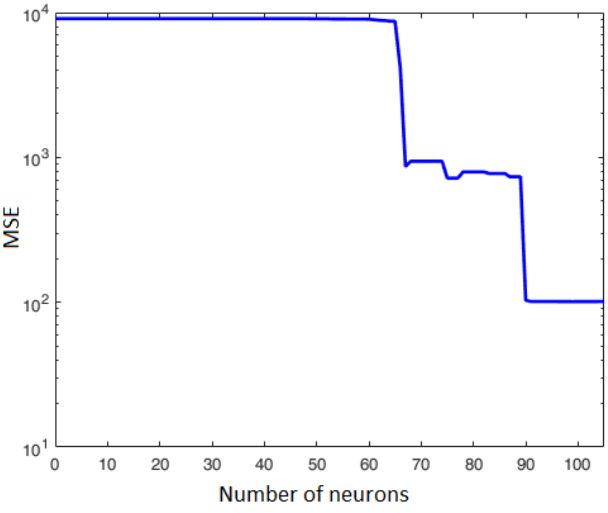

Fig. 7. Dependency between the number of neurons and MSE (resistor R_1)

The second experiment was aimed at determining the optimal width of the Gaussian activation function. The range between *0.1* and *100* was checked and the set of optimal values were was around *1* (which is usually the default value).

C. Comparison between ANN architectures

The ANN-based fault regression machine may also be based on the single network, combining available input symptoms with all diagnosed parameters (in this case 12). In this case the diagnostic module is also more compact, having much smaller number of neurons used (only in one network with the maximum number of neurons depending on the size of the training set). Unfortunately, the limited data set available for the network is not enough to train it properly. The training process converges very slowly and ends with unacceptably high MSE (the average value being around 680). Example of the training process is shown in Fig. 8. Based on the obtained results, SNA was considered as unable to accurately diagnose the RIAA filter, unless more data are added.

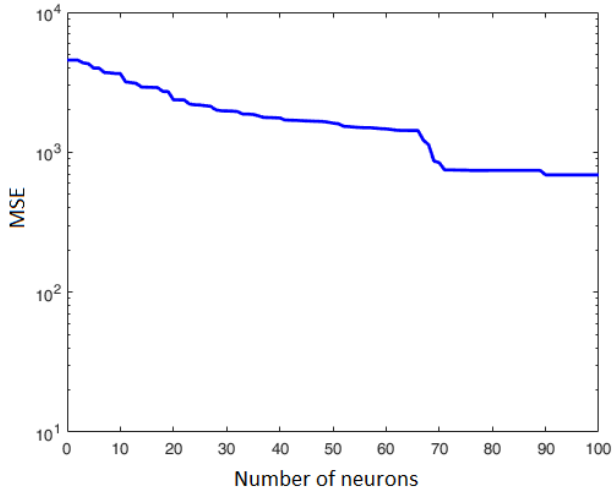

Fig. 8. Training process of the SNA

V. CONCLUSIONS

The presented research proves the RBF ANN can be used as the PI machine for the diagnostics of the RIAA correction filter. Three factors influence the regression accuracy: amount of available symptoms' vectors for training, ANN structure (the number of hidden RBF neurons) and number of symptoms allowing for distinguishing between different faults.

During the confrontation between two ANN architectures used for the task, only the more complicated INA structure has proven useful. Its advantage is especially visible in the limited data scenario, where separate approximators are able to learn at least part of the SUT parameters. Not all of them are important from the practical point of view (for instance, C_1 and R_1 are used only to cut off the DC component, so their identification is not important). Also, pairs of capacitors C_2 with C_3, and C_5 with C_6 are hardly distinguishable, because they should be treated as single elements. Therefore the obtained results are satisfactory, though additional work has to be done to improve the PI efficiency.

The future work should include application of additional approximation algorithms, introducing multiple faults and testing the approach for actual RIAA filter, which could confirm, if the available circuit models are accurate enough to diagnose the real-world systems. Also, other analog circuits (such as audio amplifiers) should be tested.

VI. ACKNOWLEDGMENTS

This work was supported by the statutory grant 504/04064/1034/40.00 from the Warsaw University of Technology.

REFERENCES

[1] **Välimäki, V., Reiss, J.D.:** All About Audio Equalization: Solutions and Frontiers, *Applied Sciences*, 2016, Vol. 6, No. 129, doi:10.3390/app6050129.

[2] **Lipshitz, S.P., Jung W.**: A High Accuracy Inverse RIAQA Network, *The Audio Amateur*, 1980, No.1, pp. 22-24.

[3] **Aminian, M. Aminian, F.**: Neural-network based analog-circuit fault diagnosis using wavelet transform as preprocessor, *IEEE Transactions on Circuits and Systems II: Analog and Digital Signal Processing*, 2000, Vol. 47, No. 2, pp. 151 – 156.

[4] LTSpice XVII(x64), Analog Devices, https://www.analog.com/en/design-center/design-tools-and-calculators/ltspice-simulator.html,

[5] **Qin, A. S. J.**: Data-driven Fault Detection and Diagnosis for Complex Industrial Processes, *IFAC Proceedings Volumes*, Vol. 42, No. 8, 2009, pp. 1115-1125.

[6] **Heo, S. Lee, J.H.**: Fault detection and classification using artificial neural networks, *IFAC-Papers OnLine*, Vol. 51, No. 18, 2018, pp. 470-475.

[7] **Yadaiah, N., Sivakumar, L., Deekshatulu, B.L.**: Parameter identification via neural networks with fast convergence, *Mathematics and Computers in Simulation*, Vol. 51, No. 3–4, 2000, pp. 157-167.

[8] **Kowalski, C.T., Kamiński, M.**: Rotor fault detector of the converter-fed induction motorbased on RBF neural network, *Bulletin of the Polish Academy of Sciences*, 2014, Vol. 62, No. 1, doi: 10.2478/bpasts-2014-0008.

[9] **Zhang, S., Zhang, S., Wang, B., Habetler T.G.**: Deep Learning Algorithms for Bearing Fault Diagnostics - A Review, *Proc. IEEE 12th International Symposium on Diagnostics for Electrical Machines, Power Electronics and Drives (SDEMPED)*, Toulouse, 27-30 Aug. 2019, doi: 10.1109/DEMPED.2019.8864915.

[10] **Bilski, P.**: Analysis of the ensemble of regression algorithms for the analog circuit parametric identification, *Measurement*, 2020, Vol. 160, doi: https://doi.org/10.1016/j.measurement.2020.107829.

.